



## Post-etch residue removal using choline chloride–malonic acid deep eutectic solvent (DES)

Jenny Taubert, Manish Keswani, Srinu Raghavan \*

Department of Materials Science and Engineering, University of Arizona, Tucson, AZ, United States

### ARTICLE INFO

#### Article history:

Available online 29 November 2011

#### Keywords:

BEOL cleaning  
Post-etch residue removal  
Deep eutectic solvent  
Electrochemical impedance spectroscopy

### ABSTRACT

Eutectic mixture of choline chloride (CC) and malonic acid (MA) in a molar ratio of 1:1 has been evaluated as a potential chemical system for the removal of residues produced by  $CF_4/O_2$  plasma etching of copper coated with DUV photoresist. Immersion cleaning was performed in the liquid at the eutectic composition at 40 and 70 °C. Residue removal rate was screened using scanning electron microscopy and verified using X-ray photoelectron spectroscopy and electrochemical impedance spectroscopy measurements. The results presented in this paper show that choline chloride–malonic acid eutectic is effective in removing post-etch residues and has the potential to function as a back end of line cleaning formulation.

© 2011 Elsevier B.V. All rights reserved.

### 1. Introduction

New process challenges arise in the semiconductor industry as device features scale down. In particular, post-etch residue removal in back end processes has become more challenging since the introduction of copper interconnect structures. New materials such as low-k and ultra-low-k (ULK) together with metal barriers and copper lines add to the complexity of the residue material generated during patterning by gas phase etching. Finding cleaning agents that are able to selectively remove these residues without corroding Cu or affecting low-k critical dimensions is a challenge in the semiconductor cleaning technology [1,2].

In BEOL processing, post-etch residues (PER) are formed during plasma etching of low-k interlayer dielectric (ILD) layers using  $CF_4$ ,  $CHF_3$  or  $C_4F_8$  in combination with  $O_2$  or Ar to form the vias and trenches for the different interconnection levels [3]. The plasma etching also exposes the underlying copper (when the nitride etch stop layer is removed) and leaves behind a polymer like residue on Cu as well as on sidewalls of dielectric [4]. The residues typically contain copper oxides, copper fluorides, and fluorocarbons among others. Effective removal of PER is of critical importance in BEOL to create good contact and adhesion between the deposited layers. The efficiency of residue removal is affected not only by the material complexity but also by where the residue is formed. Currently, semi-aqueous fluoride (SAF) cleaning formulations that contain aprotic solvents, amines, fluorides, water and in some cases, corrosion inhibitors are cleaning agents of choice in the semiconductor industry [5–8]. However, the downside of these formulations is the use of solvents that are not very environmentally friendly [9]. The

increasing interest of the industry to go “green” creates a window to replace the traditional BEOL cleaning formulations with chemicals that reduce the environmental, safety and health (ESH) impact without compromising the process performance [10,11]. In previous studies, the use of diluted HF (DHF) has been proposed as an alternative to the conventional solvent/water systems to remove PER [12,13], but the use of fluorides is a concern for health and safety [14].

Recently, a liquid mixture of two benign chemicals, choline chloride and urea, at the eutectic composition has been shown to be effective in the removal of residues formed by the  $CF_4/O_2$  etching of deep UV resist films on copper [15]. This liquid mixture belongs to a class of formulations known as deep eutectic solvents or DES but does not contain any traditional organic solvents. These formulations are ionic mixtures that are usually formed by mixing a quaternary ammonium halide salt and a hydrogen bond donor such as an amide [16], a carboxylic acid [17] or an alcohol [18]. Suitable choice of the components of DES can make them environmentally friendly formulations. During the past years several applications of DES ranging from metal extraction and biodiesel purification, to electrochemical deposition have been reported [19–21]. This large spectrum of applications is possible due to the properties of DES, such as low freezing temperature and low vapor pressure. They also have good ionic conductivity and can dissolve significant quantities of certain metal oxides and are very water soluble, which allows easy rinsing with water.

Following the preliminary work of replacing traditional solvent based formulations for PER removal with DES, the use of a system containing choline chloride (CC) mixed with malonic acid (MA) was explored. The phase diagram of the CC/MA system is shown in Fig. 1. As may be seen from this diagram, the system forms an eutectic at a 1:1 M ratio of the constituents and the eutectic

\* Corresponding author.

E-mail address: [srini@u.arizona.edu](mailto:srini@u.arizona.edu) (S. Raghavan).

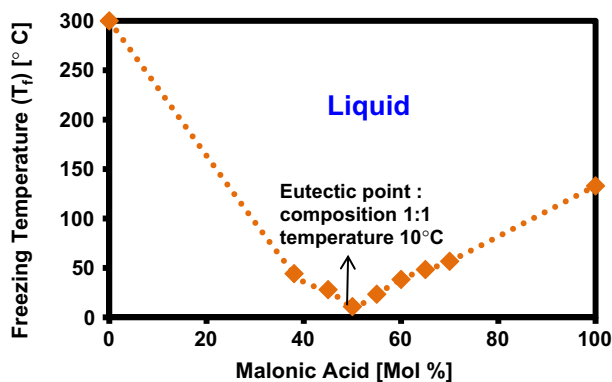


Fig. 1. Phase diagram of choline chloride/malonic acid mixtures.

temperature is 10 °C. Hence, at the room temperature, the eutectic mixture will be a liquid. Literature information indicates that the CC/MA system has a good solubility for copper oxides (18,340 ppm for cuprous oxide and 14,000 ppm for cupric oxide at 50 °C) [22]. These properties together with the green character of CC/MA liquid make it a good alternative for commercially available BEOL formulations. In this paper the feasibility of post-etch residue removal using CC/MA liquid mixture is presented.

## 2. Experimental methods

### 2.1. Post-etch residue (PER) preparation

Electroplated copper films of thickness  $\sim 1.5$   $\mu\text{m}$  provided by an integrated circuit company were pre-cleaned using isopropyl alcohol (Alfa Aesar, 99%) and 0.1 M hydrochloric acid (J.T. Baker, 96%). DUV photoresist (TDUR-P802 HP, TOK America) film of  $\sim 500$  nm in thickness was spin coated on copper film and then baked at 90 °C for 90 s. The film was then plasma etched in a reactive ion etcher (AGS) using  $\text{CF}_4/\text{O}_2$  plasma chemistry (40 sccm  $\text{CF}_4$ , 4 sccm  $\text{O}_2$ ), under 50 mTorr pressure and 250 W plasma power. Visually, the resist appeared to be etched at  $\sim 3$  min but the samples were exposed for an additional minute to ensure complete resist removal. A pre-cleaned bare copper film was exposed for 1 min to the same plasma chemistry to serve as a baseline for copper samples exposed to plasma.

### 2.2. PER film characterization

The morphology of PER films and copper films exposed to plasma was imaged using a Field Emission Scanning Electron Microscope (Hitachi S-4800) at a magnification of 100,000 $\times$ . Composition (oxidation states and bonding of elements) of the samples was analyzed by a Kratos 165 Ultra photoelectron spectrometer equipped with an Al K $\alpha$  monochromatic X-ray source. High resolution Cu 2p, C 1s, O 1s, and F 1s XPS spectra of PER film and plasma exposed copper were acquired at a pass energy of 20 eV. Charging effects were corrected by aligning all C 1s peaks to a binding energy of 284.5 eV.

### 2.3. CC/MA liquid mixture preparation

Choline chloride (CC) (Sigma,  $\geq 98\%$ ) and malonic acid (MA) (Sigma–Aldrich Reagent plus<sup>®</sup>, 99%) were mixed as received in a molar ratio of 1:1. The mixture was stirred and warmed in a double jacketed vessel at 80 °C until an amber transparent solution (CC/MA) was formed. The solution was continuously stirred upon cooling until room temperature ( $\sim 25$  °C) was reached. The viscosity of

CC/MA was measured as a function of temperature using Brookfield DV-E viscometer equipped with a thermal cell. A sample volume of 7 mL was used and the spindle was rotated in the 5 and 100 rpm range, depending on temperature. Conductivity was measured with an Orion conductivity meter equipped with a temperature compensated Orion DuraProbe 4-Electrode conductivity cell.

### 2.4. Immersion cleaning

Cleaning was performed by immersing PER samples in stirred CC/MA liquid maintained at 40 or 70 °C. Cleaning time was varied between 2 and 10 min. After cleaning the samples were thoroughly rinsed with DI water and dried with nitrogen. Plasma exposed copper samples were cleaned for 5 min in DES at 40 or 70 °C followed by rinsing with DI water and drying with nitrogen.

### 2.5. PER film removal characterization

Extent of removal of PER films was evaluated by SEM and confirmed by XPS. Further verification was obtained from Electrochemical Impedance Spectroscopy (EIS) measurements based on the method described previously [15,23]. The EIS experiments were performed using PARSTAT 2273 (Princeton Applied Research). A three electrode set up was used with PER covered Cu sample (or copper sample exposed to plasma) as the working electrode and platinum foils as quasi-reference electrode and counter electrode. The area of the working electrode exposed to the liquid was  $\sim 1$   $\text{cm}^2$ . An AC signal of 10 mV rms amplitude was applied and the frequency was swept between 100 mHz and 100 kHz. The test sequence was as follows. The sample was immersed in the DES system and at the end of 1 min of immersion, the impedance test was started. It took approximately 90 s to cover the frequency range of 100 mHz to 100 kHz. Immersion was continued for 30 s and again the impedance spectrum was taken. This process was repeated 2 more times. The data obtained are plotted as 2 and 1/2 min, 4 and 1/2 min, 6 and 1/2 min measurements. The data obtained were fitted to equivalent circuits using commercially available software ZView (Scribner Associates) to extract the electrical parameters. EIS analysis was not performed at 70 °C due to the thermal instability of malonic acid in CC/MA DES. Malonic acid decomposition is catalyzed by Pt (electrodes) at this temperature [24,25].

## 3. Results and discussion

The viscosity and conductivity of the DES system (1:1 CC:MA) is shown in Fig. 2 as a function of temperature. The conductivity is relevant for the characterization of the solvent polarity, which is important for the removal of polar residues. At room temperature, the viscosity of the liquid mixture is  $\sim 2300$  cP and the conductivity  $\sim 0.4$   $\text{mS cm}^{-1}$ . Increase of temperature from 25 to 70 °C decreases

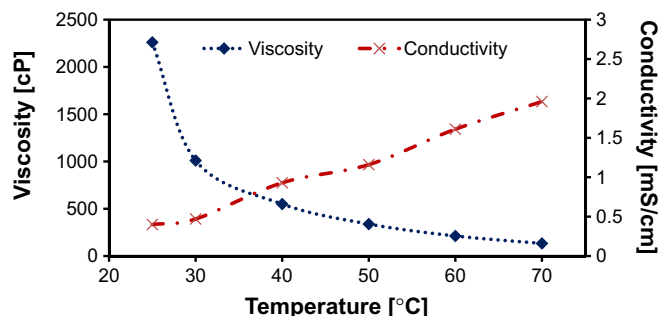


Fig. 2. Viscosity and conductivity of CC/MA liquid mixture as a function of temperature.

the viscosity by almost 20 times and increases the conductivity by almost 10-fold. Since room temperature viscosity of the liquid was very high, temperatures of 40–70 °C were chosen to perform immersion cleaning of post-etch residues. Low viscosity of cleaning fluids is very important for enhanced mass transfer of reactants and products.

The first series of tests was carried out on copper samples exposed to plasma (Cu-1 m). Scanning electron micrographs of samples before and after cleaning in the CC/MA liquid are shown in Fig. 3. Before cleaning, the plasma exposed sample shows the presence of fine (~10 nm) particulate type structures (Fig. 3a). When these samples are cleaned for 5 min in the liquid mixture maintained at 40 or 70 °C, the particulate type structures are completely removed and the surface is smooth, displaying grain structure of copper substrate (Fig. 3b and c).

Scanning electron micrograph of copper sample coated with PER shows a porous film with pores that are ~5 nm and smaller (Fig. 3d). Upon immersion cleaning for 5 min using CC/MA DES at 40 or 70 °C, the Cu surfaces are rendered residue free (Fig. 3e and f). Some level of grain boundary attack was seen at 70 °C. Incomplete residue removal was seen for cleaning times less than 5 min.

XPS analysis was used to verify if the Cu surfaces were residue free after 5 min of cleaning. A comparison of the Cu 2p, F 1s, O 1s

and C 1s spectra of PER-film, PER-film cleaned in CC/MA at 40 °C for 5 min, and Cu-1 m cleaned in CC/MA at 40 °C for 5 min is presented in Fig. 4a–d. The Cu 2p spectrum of PER is characterized by the presence of Cu 2p<sub>1/2</sub> and Cu 2p<sub>3/2</sub> main peaks at binding energies of 955 and 935 eV and shakeup satellite peaks at 961.3 and 941.5 eV respectively. These characteristics confirm that the valence state of copper in the PER film is +2. The F 1s spectrum of PER has a peak at 683.8 eV, which represents bonding of fluorine to copper in the form of CuF<sub>2</sub>. In the O 1s spectrum, the peak at 531.1 eV is due to the presence of CuO [26–29]. Based on these spectral features, it may be concluded that the PER film contains a mixture of both CuF<sub>2</sub> and CuO. In the carbon spectrum, while the prominent peak at 284.5 eV corresponds to that of C 1s, the small peak at 288 eV is most likely due to the formation of C=O from exposure to atmosphere. The presence of fluorocarbons (C<sub>x</sub>F<sub>y</sub>) was not detected in the residue; this is most likely due the fact that the resist was etched for an additional 1 min beyond the 3 min time required for its complete removal.

The effective removal of residues from PER-film cleaned in CC/MA DES is evident from the absence of fluorine peak in the F 1s spectrum. Additionally, shake-up satellite peaks in the Cu 2p spectra disappear leaving the spectrum characteristic of plasma treated copper cleaned in CC/MA. The main peaks at 931.3 and 951 eV in

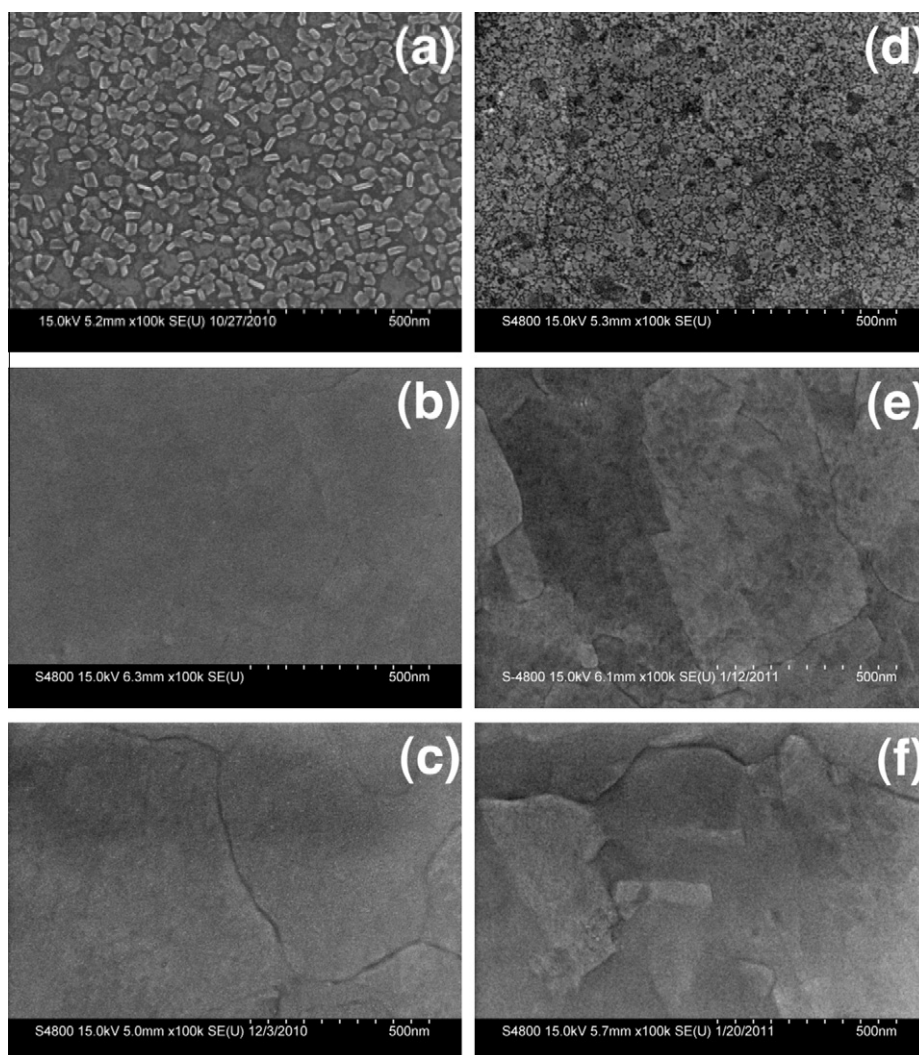


**Fig. 3.** SEM micrographs of (a) Cu exposed to CF<sub>4</sub>/O<sub>2</sub> plasma for 1 min (Cu-1 m); (b) Cu-1 m cleaned for 5 min in CC/MA liquid at 40 °C; (c) Cu-1 m cleaned for 5 min in CC/MA at 70 °C; (d) PER-film formed after ~4 min exposure to CF<sub>4</sub>/O<sub>2</sub> plasma; (e) PER-film cleaned for 5 min in CC/MA at 40 °C; (f) PER-film cleaned for 5 min in CC/MA at 70 °C.

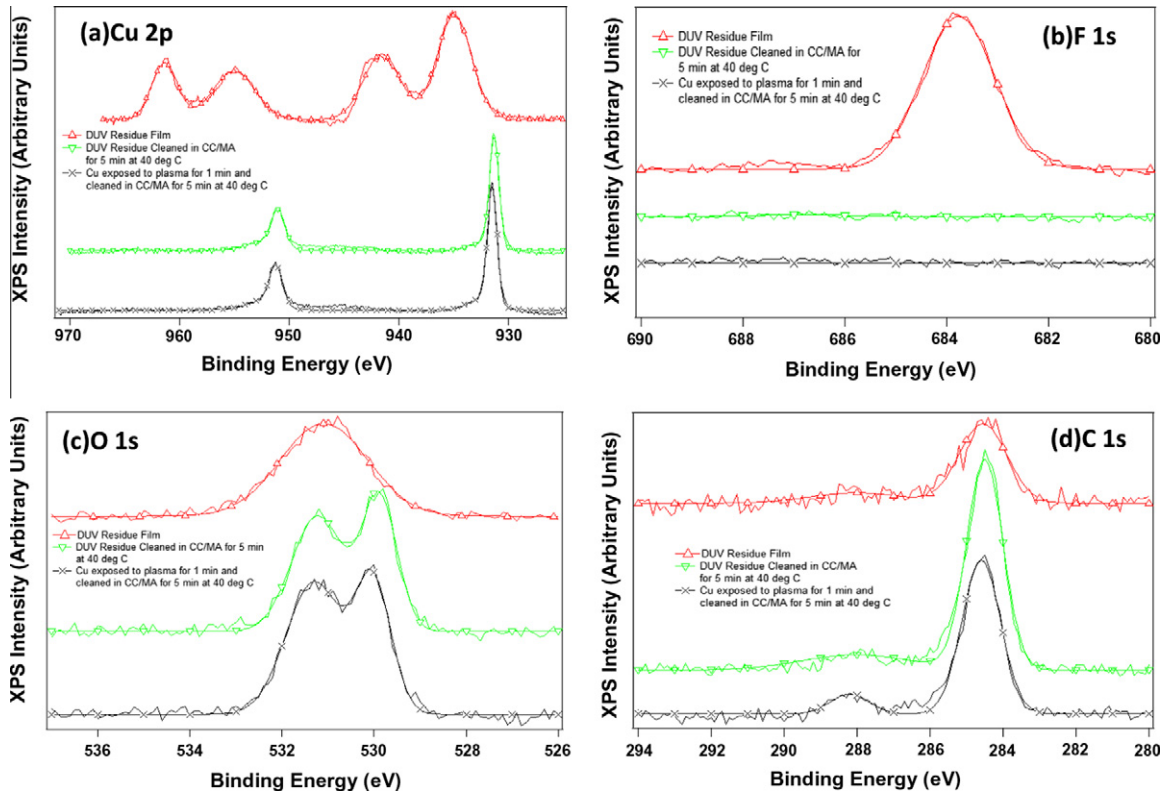


Fig. 4. Comparison of Cu 2p, F 1s, O 1s and C 1s XPS spectra of PER-film, copper exposed to plasma for 1 min (Cu-1 m), PER-film cleaned for 5 min in CC/MA at 40 °C and Cu-1 m cleaned for 5 min in CC/MA at 40 °C.

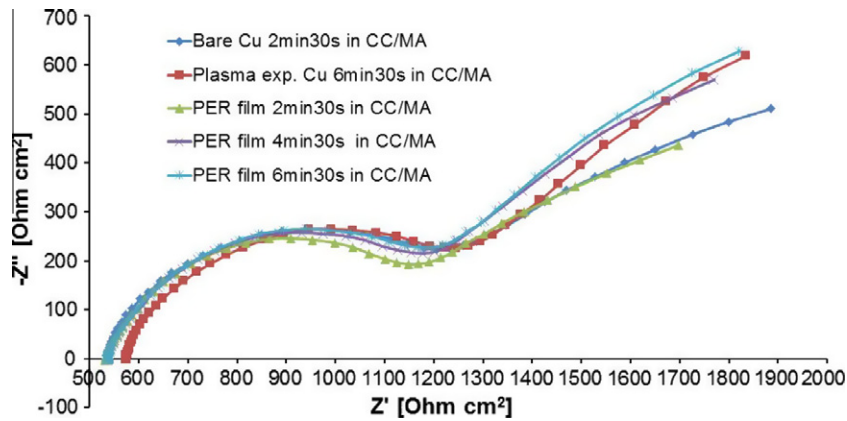


Fig. 5. Nyquist plots of Cu, Cu exposed to plasma and Cu coated with PER-film in CC/MA at 40 °C as a function of time.

the Cu 2p spectrum are those for elemental copper whereas shoulders at 952.5 and 932.5 eV are related to native oxides of Cu (+1) formed during atmospheric exposure. The presence of Cu (+1) is also confirmed by a peak at 529.9 eV in the O 1s spectrum. The peak at 531.2 eV might be associated with C=O due to exposure to contaminants from atmosphere [30]. For the C 1s spectrum, no significant change in the peak position was observed.

EIS measurements on PER film coated Cu, plasma exposed Cu and bare copper samples were made in CC/MA liquid at 40 °C to confirm residue removal. Impedance spectra were collected for each sample as a function of time. Nyquist plots obtained from the PER-film coated Cu sample are shown as an example in Fig. 5. In all the plots a depressed semi-circle is observed. This kind of arc depression is usually due to surface inhomogeneities in the electrode-material system [31]. A characteristic finite length War-

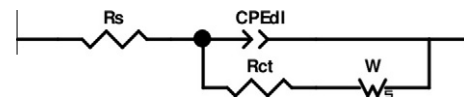


Fig. 6a. Randle circuit model with mass transport limitations to fit impedance data obtained on Cu sample immersed in CC/MA DES at 40 °C.

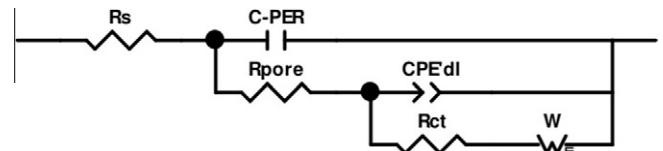


Fig. 6b. Equivalent circuit model to fit impedance data collected on PER-film coated Cu and Cu-1 m sample in CC/MA DES at 40 °C.



**Table 1**

Electrical parameters obtained by fitting Nyquist plots of Cu, PER-film and Cu exposed to plasma in CC/MA liquid mixture at 40 °C as a function of time. Diffusion layer length *L* is reported at the bottom of the table.

|   | Cu                | PER-film          | Cu-1 m            |                 |                   |                   |                   |
|---|-------------------|-------------------|-------------------|-----------------|-------------------|-------------------|-------------------|
| Time range [min]                                    | 2 and 1/2         | 2 and 1/2         | 4 and 1/2         | 6 and 1/2       | 2 and 1/2         | 4 and 1/2         | 6 and 1/2         |
| $R_s$ [ $\Omega$ ]                                  | 530 ± 6           | 539 ± 2           | 542 ± 2           | 543 ± 1         | 531 ± 47          | 533 ± 47          | 531 ± 47          |
| C-PER [ $\mu$ F]                                    | –                 | 5.9 ± 0.4         | 6.0 ± 0.3         | –               | 5.6 ± 0.7         | 5.7 ± 0.7         | –                 |
| $R_{pore}$ [ $\Omega$ ]                             | –                 | 114 ± 2           | 152 ± 1           | –               | 137 ± 4           | 185 ± 3           | –                 |
| $CPE'_{dl-T}$ [ $\mu$ F s <sup>(<i>P</i>-1)</sup> ] | –                 | 29.3 ± 0.9        | 22.9 ± 2.1        | –               | 31.9 ± 2.7        | 25.6 ± 2.6        | –                 |
| $CPE''_{dl-P}$                                      | –                 | 0.84 ± 0.01       | 0.89 ± 0.01       | –               | 0.81 ± 0.03       | 0.86 ± 0.03       | –                 |
| $CPE_{dl-T}$ [ $\mu$ F s <sup>(<i>P</i>-1)</sup> ]  | 29.5 ± 2.0        | –                 | –                 | 22.9 ± 1.7      | –                 | –                 | 24.3 ± 0.9        |
| $CPE_{dl-P}$  | 0.80 ± 0.01       | –                 | –                 | 0.85 ± 0.01     | –                 | –                 | 0.83 ± 0.01       |
| $R_{ct}$ [ $\Omega$ ]                               | 758 ± 154         | 387 ± 50          | 348 ± 53          | 492 ± 39        | 462 ± 44          | 411 ± 35          | 615 ± 57          |
| $W-R$ [ $\Omega$ ]                                  | 1611 ± 155        | 981 ± 137         | 1494 ± 123        | 1952 ± 91       | 1027 ± 108        | 1548 ± 78         | 1877 ± 294        |
| $W-T$ [s]   | 4.9 ± 0.6         | 4.2 ± 0.5         | 6.3 ± 0.2         | 8.5 ± 0.5       | 4.2 ± 0.8         | 6.6 ± 0.8         | 8.5 ± 2.4         |
| $W-P$   | 0.44 ± 0.01       | 0.43 ± 0.01       | 0.45 ± 0.01       | 0.44 ± 0.0      | 0.44 ± 0.01       | 0.44 ± 0.01       | 0.46 ± 0.01       |
| $\chi^2$  | 0.00042 ± 0.00001 | 0.00029 ± 0.00006 | 0.00042 ± 0.00002 | 0.0011 ± 0.0003 | 0.00027 ± 0.00009 | 0.00033 ± 0.00005 | 0.00076 ± 0.00003 |
| <i>L</i> [ $\mu$ m]                                 | 1.97              | 1.82              | 2.24              | 2.61            | 1.84              | 2.29              | 2.60              |

burg diffusion response is observed as well. This indicates that there are mass transfer limitations in this high viscosity system.

The impedance spectra of bare copper were fitted to a typical Randle circuit with mass transport limitations shown in Fig. 6a, whilst the spectra of copper exposed to plasma and PER-film samples were fitted to an equivalent circuit shown in Fig. 6b. In these models  $R_s$  corresponds to the resistance of the DES liquid,  $R_{ct}$  to the charge transfer resistance at the Cu/DES interface,  $R_{pore}$  represents the pore resistance in the film,  $W_s$  is the Warburg diffusion element of finite length,  $CPE_{dl}$  and  $CPE'_{dl}$  represent constant phase elements associated with the double layer capacitance at the Cu/electrolyte and PER coated Cu/electrolyte interfaces, and C-PER is the capacitance of the PER film. The impedance of  $W_s$  (Eq. (1)) is defined as:

$$Z_{W_s} = R \times \tanh[(j\omega T)^P] / (j\omega T)^P \tag{1}$$

where the parameter *R* corresponds to the Warburg element resistance related to the diffusion of the electroactive species. The term (*jω*) is the product of *j*, an imaginary number equal to  $\sqrt{-1}$ , and  $\omega$ , which is  $2\pi$  times the linear frequency. The parameter *T* is related to the length of the diffusion layer *L* and to the diffusion coefficient *D* through the relationship,  $T = (L^2/D)$ , and *P* is an exponent related to the slope of linear part in the Nyquist plot.

The impedance of constant phase elements, CPE, is defined as:

$$Z_{CPE} = 1/[T \times (j\omega)^P] \tag{2}$$

In the above equation, *T* is the capacitance value of the CPE, which is essentially a distributed capacitor and the exponent *P* is related to the surface roughness/inhomogeneity. CPE behaves like a pure capacitor when *P* = 1.

The electrical parameters obtained from the fit of experimental data to the models are given in Table 1. As the PER film gets removed, the value of C-PER is expected to increase since C-PER is inversely proportional to PER thickness. The best fit values of the circuit parameters of Cu-1 m and PER-film as a function of time indicate that C-PER remains almost constant in the time, perhaps due to the fast removal rate of PER in CC/MA. Another circuit parameter used to analyze PER removal is the double layer capacitance of PER-film, Cu-1 m and Cu. Past studies [15,23] indicated that the value of PER-film double layer capacitance ( $CPE'_{dl-T}$ ) increased with immersion time approaching the value of double layer capacitance of Cu ( $CPE_{dl-T}$ ). Increase in the  $CPE'_{dl-T}$  value was explained by the increase of Cu area exposed to electrolyte as PER-film dissolved. In the case of PER-film and Cu-1 m removal in CC/MA the best fit values of  $CPE'_{dl-T}$  and  $CPE_{dl-T}$  indicate that both values are almost the same after a short period of time (Table 1). An apparent decrease is observed as well, however the variation is not significant ( $\sim 10 \mu$ F) and over a longer period of time

the values appear to remain constant. The behavior of  $CPE_{dl-T}$  as a function of time indicates a fast PER removal kinetics without formation of a passive layer. The later can be observed as well in the  $R_{ct}$  values, which remain constant over time. One note of interest is that the charge transfer resistance ( $R_{ct}$ ) of plasma exposed copper is lower than that of bare copper by  $\sim 300 \Omega$ , indicating that copper exposed to plasma is more prone to corrode.

The fitted values of the parameters, *R*, *P* and *T* in the Warburg element, are represented by *W-R*, *W-T* and *W-P* in Table 1. Diffusion layer thickness (*L*) values were calculated from fitted *W-T* values and diffusion coefficient of ions in DES and are also tabulated in Table 1. The calculated diffusion layer thicknesses are of the order of microns, which are of the right order of magnitude for liquids with a viscosity in the neighborhood of 100 cP. This lends support to the goodness of fit of the impedance data.

Cleaning rate can be calculated from the film thickness divided by the removal time. The thickness of PER films used in this investigation was  $\sim 17$  nm, as measured by atomic force microscopy. SEM and EIS measurements indicate that the PER film is removed within 5 min; based on this that a cleaning rate of  $\sim 30 \text{ \AA min}^{-1}$  may be calculated. This removal rate is faster than that obtained using choline chloride/urea (CC/U) liquid mixtures [15]. The higher removal rate in CC/MA system may be attributed to the higher solubility of copper oxides in CC/MA [22].

**4. Conclusions**

Liquid mixtures consisting of choline chloride (CC) and malonic acid (MA) in a molar ratio of 1:1 were effective in removing residues formed by  $CF_4/O_2$  plasma etching of copper coated with DUV-photoresist. X-ray photoelectron spectroscopy (XPS) characterization showed that PER film contains a mixture of copper fluorides and copper oxides. The residues were effectively removed at a rate of  $\sim 30 \text{ \AA min}^{-1}$  at 40 °C.

**Acknowledgements**

The authors would like to acknowledge the financial support from SRC/Sematech Engineering Research Center for Environmentally Benign Manufacturing at The University of Arizona through contract #2001-MC-424. The authors would like also to acknowledge fruitful discussions with Mr. Dinesh Thanu, whose previous work on CC/U DES created the basis for this project.

**References**

[1] M. Engelhardt, G. Schindler, W. Steinhoegl, G. Steinlesberger, Microelectronic Engineering 64 (2002) 3–10.

- [2] K. Mosig, T. Jacobs, K. Brennan, M. Rasco, J. Wolf, R. Augur, *Microelectronic Engineering* 64 (2002) 11–24.
- [3] H. Abe, M. Yoneda, N. Fujiwara, *Japanese Journal of Applied Physics* 47 (3) (2008) 1435–1455.
- [4] D. Louis, C. Payne, E. Lajoinie, B. Vallesi, D. Holmes, D. Maloney, S. Lee, *Microelectronic Engineering* 46 (1999) 307–310.
- [5] C.F. Tsang, C.K. Chang, A. Krishnamoorthy, K.Y. Ee, Y.J. Su, H.Y. Li, W.H. Li, L.Y. Wong, *Microelectronics Reliability* 45 (2005) 517–524.
- [6] G.W. Gale, R. Small, K.A. Reinhardt, in: K.A. Reinhardt, W. Kern (Eds.), *Handbook of silicon wafer cleaning technology*, second ed., William Andrew Inc., New York, 2008, pp. 201–265.
- [7] N.H. Kim, S.Y. Kim, H-K. Lee, K-Y. Lee, C.I. Kim, E.G. Chang, *Journal of Vacuum Science and Technology B* 25 (6) (2007) 1819–1822.
- [8] Q.T. Le, M. Claes, T. Conard, E. Kesters, M. Lux, G. Vereecke, *Microelectronic Engineering* 86 (2009) 181–185.
- [9] P. Singer, *Semiconductor International* (2007) 38–40.
- [10] A. Hand, *Semiconductor International* (2008) 24–30.
- [11] M. Avalos, R. Babiano, P. Cintas, J.L. Jimenez, J.C. Palacios, *Angewandte Chemie International Edition* 45 (2006) 3904–3908.
- [12] D.P.R. Thanu, S. Raghavan, M. Keswani, *Journal of the Electrochemical Society* 158 (2011) 814–820.
- [13] K. Ueno, V.M. Donnelly, T. Kikkawa, *Journal of the Electrochemical Society* 144 (1997) 2565–2572.
- [14] L. Peters, *Video Business* (2002) 57–62.
- [15] D.P.R. Thanu, S. Raghavan, M. Keswani, *Electrochemical and Solid State Letters* 14 (2011) 358–361.
- [16] A.P. Abbott, G. Capper, D.L. Davies, R.K. Rasheed, V. Tambyrajah, *Chemical Communications* (2003) 70–71.
- [17] A.P. Abbott, D. Boothby, G. Capper, D.L. Davies, R. Rasheed, *Journal of the American Chemical Society* 126 (2004) 9142–9147.
- [18] R.C. Harris, Ph.D. Dissertation, Department of Chemistry, University of Leicester, 2008.
- [19] A.P. Abbott, G. Capper, D.L. Davies, R.K. Rasheed, P. Shikotra, *Inorganic Chemistry* 44 (2005) 6497–6499.
- [20] A.P. Abbott, P.M. Cullis, M.J. Gibson, R.C. Harris, E. Raven, *Green Chemistry* 9 (2007) 868–872.
- [21] A.P. Abbott, K. El Ttaib, G. Frisch, K.J. McKenzie, K.S. Ryder, *Physical Chemistry Chemical Physics* 11 (2009) 4269–4277.
- [22] A.P. Abbott, G. Capper, D.L. Davies, K.J. McKenzie, S.U. Obi, *Journal of Chemical and Engineering Data* 51 (2006) 1280–1282.
- [23] N. Venkataraman, S. Raghavan, *Microelectronic Engineering* 87 (2010) 1689–1695.
- [24] H.Z. Jakubowicz, *Anorganische Allgemeine Chemie* 121 (1922) 113–127.
- [25] Z.P.G. Masende et al., *Applied Catalysis B: Environmental* 56 (2005) 189–199.
- [26] C.D. Wagner, A.V. Naumkin, A.K. Vass, J.W. Allison, C.J. Powell, J.R. Rumble, NIST X-ray Photoelectron Spectroscopy Database. <<http://www.srdata.nist.gov/xps/>>.
- [27] J. Kawai, K. Maeda, K. Nakajima, *Physical Review B* 48 (12) (1993) 8560–8566.
- [28] Y.W. Zhu, A.M. Moo, T. Yu, X.J. Xu, X.J. Gao, Y.J. Liu, C.T. Lim, Z.X. Shen, C.K. Ong, A.T.S. Wee, J.T.L. Thong, C.H. Sow, *Chemical Physical Letters* 419 (2006) 458–463.
- [29] J. Ghijsen, H. Tjeng, J. van Elp, H. Eskes, J. Westerink, G.A. Sawatzky, *Physical Review B* 38 (16) (1988) 322–330.
- [30] S. Poulston, P.M. Parlett, P. Stone, M. Bowker, *Surface and Interface Analysis* 24 (1996) 811–820.
- [31] E. Barsoukov, J.R. Macdonald, *Impedance Spectroscopy – Theory, Experiment and Applications*, second ed., John Wiley and Sons Inc., New Jersey, 2005.